J Neurophysiol 131: 106–123, 2024.
First published December 13, 2023; doi:10.1152/jn.00086.2023

american physiological society

JNP JOURNAL OF NEUROPHYSIOLOGY

RESEARCH ARTICLE

Control of Movement

Reversible deactivation of motor cortex reveals that areas in parietal cortex are differentially dependent on motor cortex for the generation of movement

Chris S. Breese,[1]* Dylan F. Cooke,[2,3]* Adam B. Goldring,[1,4] Mary K. L. Baldwin,[1,4] Carlos R. Pineda,[1,4] and Leah A. Krubitzer[1,4]

[1]*Center for Neuroscience, University of California, Davis, California, United States;* [2]*Department of Biomedical Physiology and Kinesiology, Simon Fraser University, Burnaby, British Columbia, Canada;* [3]*Institute for Neuroscience & Neurotechnology, Simon Fraser University, Burnaby, British Columbia, Canada; and* [4]*Department of Neurology, University of California Davis, California, United States*

Abstract

Primates are characterized by specializations for manual manipulation, including expansion of posterior parietal cortex (PPC) and, in Catarrhines, evolution of a dexterous hand and opposable thumb. Previous studies examined functional interactions between motor cortex and PPC in New World monkeys and galagos, by inactivating M1 and evoking movements from PPC. These studies found that portions of PPC depend on M1 to generate movements. We now add a species that more closely resembles humans in hand morphology and PPC: macaques. Inactivating portions of M1 resulted in all evoked movements being reduced (28%) or completely abolished (72%) at the PPC sites tested (in areas 5L, PF, and PFG). Anterior parietal area 2 was similarly affected (26% reduced and 74% abolished) and area 1 was the least affected (12% no effect, 54% reduced, and 34% abolished). Unlike previous studies in New World monkeys and galagos, interactions between both nonanalogous (heterotopic) and analogous (homotopic) M1 and parietal movement domains were commonly found in most areas. These experiments demonstrate that there may be two parallel networks involved in motor control: a posterior parietal network dependent on M1 and a network that includes area 1 that is relatively independent of M1. Furthermore, it appears that the relative size and number of cortical fields in parietal cortex in different species correlates with homotopic and heterotopic effect prevalence. These functional differences in macaques could contribute to more numerous and varied muscle synergies across major muscle groups, supporting the expansion of the primate manual behavioral repertoire observed in Old World monkeys.

NEW & NOTEWORTHY Motor cortex and anterior and posterior parietal cortex form a sensorimotor integration network. We tested the extent to which parietal areas could initiate movements independent of M1. Our findings support the contention that, although areas 2, 5L, PF, and PFG are highly dependent on M1 to produce movement, area 1 may constitute a parallel corticospinal pathway that can function somewhat independently of M1. A similar functional architecture may underlie dexterous tool use in humans.

area 2; area 5; frontoparietal network; intracortical microstimulation; M1

INTRODUCTION

One of the hallmarks of human evolution is our dexterous hands. Our early ancestors used their hands to produce stone tools that ultimately led to the technology, tools, and architectural wonders that define the modern human condition. However, our hands and the cortical networks that generate our remarkable manual behaviors did not evolve de novo in humans. Rather, aspects of hand morphology and some of the cortical areas associated with motor control of the hands emerged relatively early in primate evolution, and some likely before the emergence of primates (see Refs. 1 and 2 for review). Comparative studies in primates such as galagos, owl monkeys, and squirrel monkeys indicate that there is a strong anatomical (3, 4) and functional (5, 6) relationship between cortical areas involved in the planning (e.g., PPC)

*C. S. Breese and D. F. Cooke contributed equally to this work.
Correspondence: L. A. Krubitzer (lakrubitzer@ucdavis.edu).
Submitted 28 February 2023 / Revised 12 December 2023 / Accepted 13 December 2023

and execution (e.g., motor/premotor cortex) of hand movements. Specifically, in prosimian galagos and New World monkeys, areas in PPC are strongly connected with motor areas in frontal cortex and are dependent on motor cortex (M1) for the generation of movements evoked using intracortical microstimulation (ICMS). The anatomical connections (7–18), as well as the complex sensory-motor integration and movement control properties (19–28) of PPC, have been extensively examined in Old World macaque monkeys. However, the hierarchical, parallel, or independent relationship of PPC with classically defined M1 has not been well established. Investigating the nature of this relationship is important because, compared with prosimians and New World monkeys, macaques' hand morphology and manual dexterity more closely resemble those of humans. Furthermore, PPC has expanded and is composed of multiple cortical fields in Old World macaque monkeys [a lineage more closely related to humans) compared with other primates studied (see Ref. 1 for review)].

Anterior parietal cortical areas (3a, 3 b/S1,1 and 2) have been explored using long train ICMS techniques in a variety of primates (29–31), tree shrews (32), rodents such as mice and rats (33, 34), and recently in bats (35). All of these studies demonstrate that movements can be evoked from somatosensory cortex, even independently of M1 in mice (36), with control of certain movements divided between M1 and S1 (33, 34). These data suggest that there may be two parallel motor control pathways, at least in rodents, and this supposition is supported by the strong corticospinal projections from S1 in rodents (37, 38).

However, although primates have corticospinal connections from areas in anterior and posterior parietal cortex (9, 10, 27), it is not clear if they have an independent motor control pathway such as may exist in rodents. In primates (particularly macaques), the number of anterior parietal fields is substantially greater than in mice, and the anatomical connections between somatosensory and motor cortex in rodents and primates are dramatically different. Specifically, S1 in mice and rats has dense projections with motor cortex (39–41), whereas S1 (area 3 b) in primates has few to no direct connections with motor cortex (18, 42, see Ref. 69 for review).

Although others have extensively investigated anatomical connections of the frontoparietal network, as well as the function of motor and parietal cortex during behavior, here we investigate the functional relationship between M1 and posterior parietal and anterior parietal cortical areas using ICMS techniques coupled with reversible deactivation. Specifically, we examined the effects of reversibly deactivating M1, via cooling, on evoked movements in areas 1, 2, 5L, PF, and PFG. We sought to determine the extent to which evoked movements in these fields were dependent upon M1, and to investigate the functional convergence and divergence between specific movement representations in M1 with those in anterior and posterior parietal areas. We also compared the effects of cooling movement representations in M1 that were analogous (homotopic) versus nonanalogous (heterotopic) to movements evoked from stimulation sites in anterior and posterior parietal cortex. We discuss our results in light of findings from similar experiments in other species and in relation to differences in functional motor maps across diverse mammalian species.

MATERIALS AND METHODS

In three adult macaque monkeys (1 male and 2 females) ranging from 5.3–9.6 kg and ages 7–14 yr, we examined the effect of deactivating motor cortex on evoked movements in parietal cortex (Fig. 1, *A–C*). One additional macaque monkey was used to examine the cooling properties and cooling footprint of our cooling chips. All procedures were approved by the UC Davis Institutional Animal Care and Use Committee (IACUC) and followed National Institutes of Health (NIH) guidelines.

Surgical Procedures

Detailed surgical procedures have been described in a previous study (29). Briefly, anesthesia was induced with ketamine hydrochloride (20–39 mg/kg, im) and then maintained with isoflurane anesthesia (2%) throughout surgery. Heart rate, respiration rate, O_2 saturation, body temperature, muscle tone, and reflexes were monitored throughout the experiment to ensure a constant level of anesthesia. To confirm the stability of anesthesia, and therefore our ability to consistently evoke movements, throughout the experiment, we periodically returned to stimulation sites to retest the minimum stimulation level that could evoke a response. Animals were placed in a stereotaxic frame and positioned such that their upper trunk and forelimbs were unobstructed. A craniotomy was made to expose portions of frontal and parietal cortex. Once the dura was removed, liquid silicone was placed over the cortex to prevent desiccation. An image of the cortical surface was captured and printed so that stimulation site locations could be recorded relative to cortical vascular patterns and sulcal landmarks. Following completion of the craniotomy, we transitioned anesthesia to intravenous ketamine (25–35 mg/kg/h) and supplemental intramuscular xylazine injections (1 mg/kg).

ICMS Mapping

A full description of movement maps in these monkeys has been reported previously (29). Data collection started with an exploration of movement representations in frontal and parietal cortex. We elicited movements from stimulation sites in area 1, area 2, PF, PFG, and 5L. The stimulation electrode was lowered 1,800 μm into the cortex, corresponding to the depth of cortical layers V and VI. In the banks of sulci, the electrode was advanced perpendicular to the pial surface and stimulation was administered every 500 μm up to a maximum depth of 6 mm. Electrical stimulation consisted of 500-ms trains of biphasic pulses (each phase 0.2 ms in duration) delivered at 200 Hz. If no movement was detected for amplitudes of up to 600 μA, the site was considered to be nonexcitable. We defined an "excitation threshold" as the excitation current intensity at which an evoked movement could be elicited ~50% of the time, or a value (e.g., 12.5 μA) between an intensity that could evoke movements all of the time (e.g., 15 μA) and an intensity at which no movements could be evoked (e.g., 10 μA). This is a commonly used criteria for determining excitation threshold (see Refs. 32, 46–48 for examples). Excitation thresholds for each area were as follows (mean ± standard deviation): area 1, 239 ± 147 μA; area 2, 272 ± 135 μA; area 5L, 400 ± 185 μA; area PF, 383 ± 38 μA; and area PFG, 273 ± 118 μA. Subsequent stimulation, for the purpose of assessing response at baseline and during testing, was done at a higher

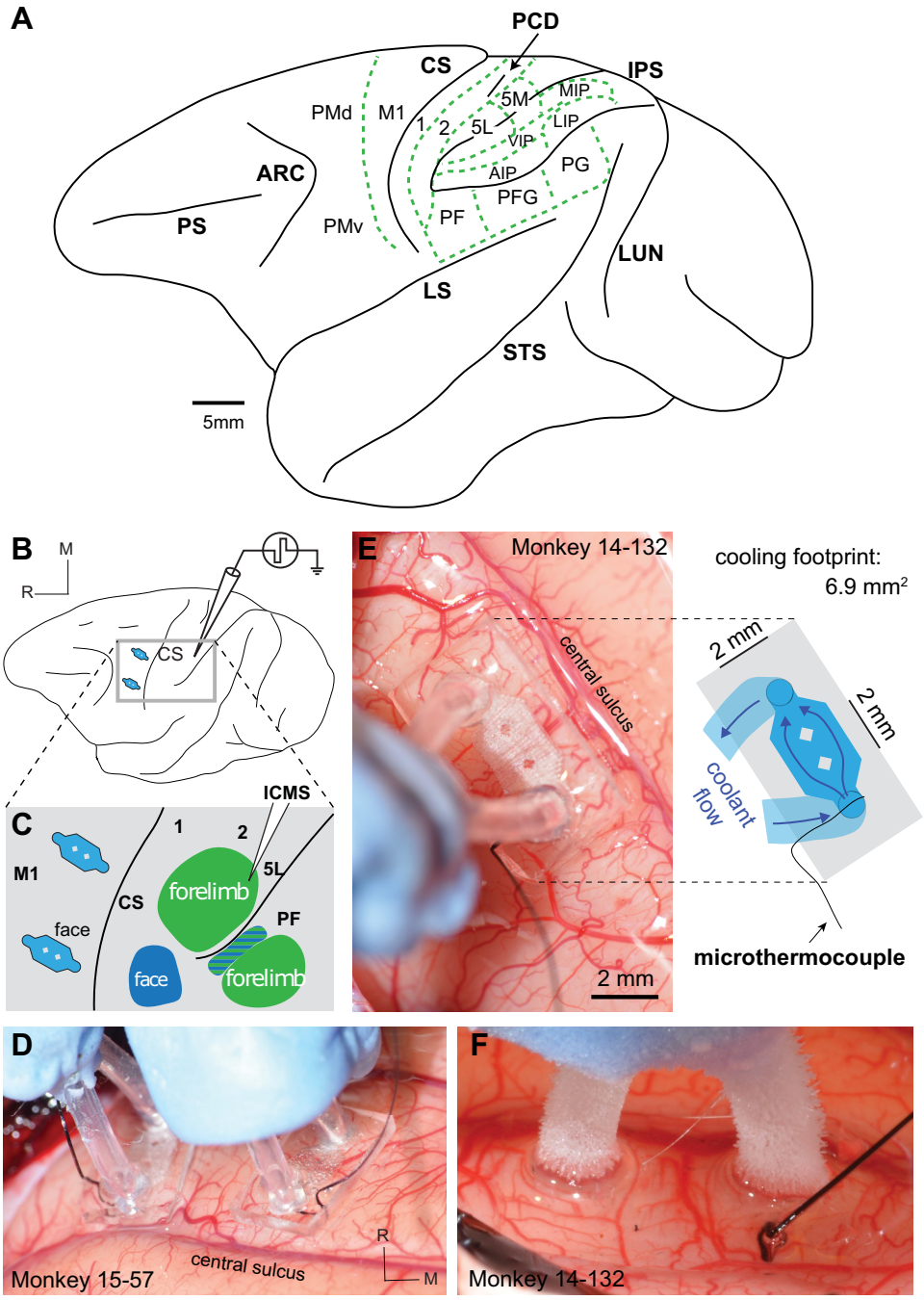

Figure 1. *A*: lateral view of the macaque monkey brain showing the location of cortical fields in motor, somatosensory, and posterior parietal cortex (delineated by green dashed lines) relative to major sulci (solid black lines). In this view, the intraparietal sulcus (IPS) has been opened. The divisions of posterior parietal cortex are derived from a number of studies (8, 9, 28, 44, 45). However, the nomenclature, function, and relative location of areas in the PPC often differs between laboratories. *B–F*: experimental set-up and cooling chip placement. *B*: schematic of the brain with two cooling chips placed in M1, and a stimulating electrode in parietal cortex. *C*: expansion of the box in *B* showing stimulation of the forelimb movement representation (green) in parietal cortex. Stimulation of the forelimb representation in area 2 while cooling the M1 forelimb representation would be a test of homotopic functional interactions; stimulation in the same location in area 2 during cooling of the face representation in M1 would be a test of heterotopic functional interactions. *D*: photograph of cooling chips in Monkey 15-57, schematized in *B* and *C*, imaged from a different aspect (medial is right and rostral is to the top). Blue dental acrylic connects each cooling chip to a wire secured to a micromanipulator. *E*: cooling chip from monkey 14-132 viewed from above. In this image, medial (M) is to the top, and rostral (R) is to the left. The schematics to the right show coolant flow through the light blue tubing and the dimensions of the cooling chamber (darker blue, "cooling footprint"). *F*: rostral view of the cooling chip shown in *E* during a cooling epoch. Black wires in *D–F* are 44-gauge microthermocouples measuring temperature at the interface between the cooling chip and the brain. This thermal feedback was used to regulate and maintain temperature by adjusting coolant flow. AIP, anterior intraparietal area; ARC, arcuate sulcus; CS, central sulcus; IPS, intraparietal sulcus; LIP, lateral intraparietal area; LS, lateral sulcus; LUN, lunate sulcus; M1, primary motor cortex; MIP, medial intraparietal area; PCD, postcentral dimple; PF, rostral inferior parietal lobule; PFG, medial inferior parietal lobule; PG, caudal inferior parietal lobule; PMd, dorsal premotor cortex; PMv, ventral premotor cortex; PS, principal sulcus; STS, superior temporal sulcus; VIP, ventral intraparietal area.

J Neurophysiol • doi:10.1152/jn.00086.2023 • www.jn.org

amplitude. The average stimulation current used for testing was as follows (mean ± standard deviation): area 1, 529 ± 143 μA; area 2, 482 ± 144 μA; area 5L, 600 ± 0 μA; area PF, 600 ± 0 μA; and area PFG, 600 ± 0 μA. To ensure that the electrode delivered consistent current, we monitored the amplitude of the waveform concurrently, measuring stimulation current by the voltage drop across a 10-kΩ resistor in series with the return lead of the stimulation isolation units. The waveform was also recorded from the stimulation electrode via Spike II (Cambridge Electronic Design Limited). All movements were digitally recorded from two angles (60 frames/s) and analyzed off-line (see *Movement Analysis*). Fiducial probes (fluorescent dyes) were placed at strategic locations within cortex to align functional and histological data.

Cooling Chips

Microfluidic thermal regulators, or "cooling chips," which contain an integrated microthermocouple to record temperature at the chip/brain interface, were custom fabricated from polydimethylsiloxane (PDMS) and silicone tubing. The properties of these devices have been described previously (49), and the current, more compact design used here has also been described [(43, 50) Fig. 1, *D* and *E*]. In these cooling chips, ethanol coolant flows through a laser-cut chamber separated from the cortical surface by a 100-μm PDMS membrane. This chamber defines the direct cooling footprint of 6.8 mm^2. Coolant flow is regulated to maintain a hypothermic target temperature in adjacent cortex. Cooling chips with a smaller cooling footprint but otherwise identical design have been used in galagos (5).

In these cooling chips, temperature was measured at the cortical surface via microthermocouples integrated into the cooling chip. Because heat transfer drops off dramatically with distance from the cortical surface (approaching normal cortical temperatures at depths of 3,000 μm and 500 μm lateral), the underlying white matter was unlikely to be exposed to temperatures that would affect activity (49). Though cooling extent (both depth and breadth) and consistency of such chips have been described in multiple species (see Ref. 49, Figs. 9 and 12), we replicated these measurements with the current chips. To test the lateral extent of cooling, we collected thermographic data (Fig. 2, *A*–*D*) on identical cooling chips in an additional macaque monkey that was not part of this ICMS/cooling study. To gather these thermographic data,

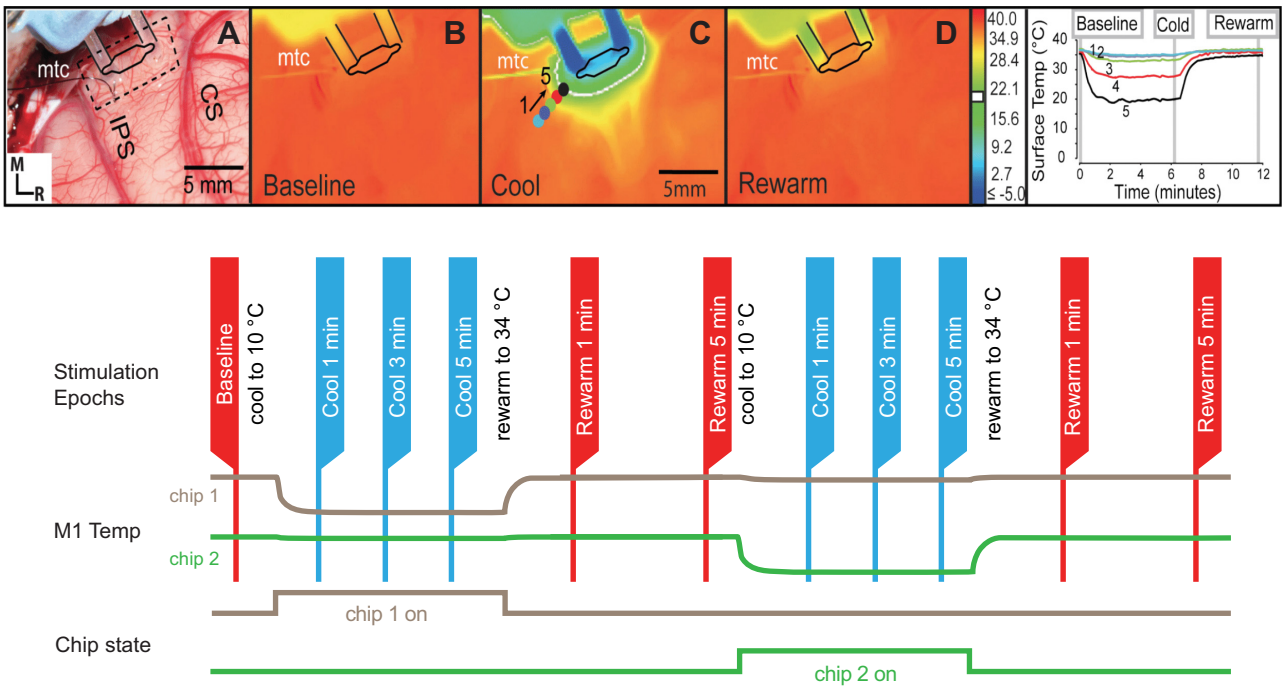

Figure 2. *Top*: thermography during cortical cooling. To examine the cooling profile of our chips, a cooling chip was placed over areas 2 and 5 M. *A*: the outline (dashed rectangle) of the PDMS base is larger than the cooling channel (solid outline on cortex). Thermal images from matching perspective depicting cortex temperature prior to (*B*), during (*C*), and after cooling (*D*). Inflow and outflow tubes are outlined in black. Cortical temperature throughout the three epochs was also measured by a microthermocouple (mtc) under the device. The very cold temperatures (dark blue) in *C* are the coolant in the inflow and outflow tubes, not the cortical surface below the chip. A temperature scale is shown to the right of *D* and the deactivation isotherm (19–21°C) is indicated by a white square, which is also highlighted as a white ring during cooling (*C*). The temperature scale shows the time course of the thermal data from 5 pixels marked by colored circles in *C* at increasing 0.75-mm intervals from the cooling chip. The timing of the 3 frames (*B*–*D*) is shown by vertical gray lines on the plot. Cortical temperatures were stable within 1–2 min of cooling. *Bottom*: temporal sequence of data collection for each intracortical microstimulation (ICMS) site tested during cooling. For each cooling chip, data were collected from up to six stimulation epochs marked by red and blue flags. Cooling chips were activated at separate times (bottom square wave traces) while temperature on the M1 surface was measured (middle traces). Before cooling of chip 1, Baseline Epoch (red flag at left) ICMS movements were recorded on video. Chip 1 (brown traces) was then activated, and ICMS movements were again video recorded during up to 3 cooling epochs (blue flags) 1, 3, and 5 min after the time when cortex reached 10°C. If movements were abolished at 1 or 3 min, subsequent cooling epochs were not performed. Chip 1 was then turned off and ICMS movements were video recorded during rewarm epochs (red flags at center) 1 and 5 min after cortex temperature warmed passively to 34°C. Excitation thresholds were measured during Baseline, Cool 5, Rewarm 1, and Rewarm 5 Epochs. In monkeys with a second cooling chip, this cycle was repeated with the chip 1, Rewarm 5 Epoch serving as the Baseline Epoch for chip 2 (green traces). PDMS, polydimethylsiloxane.

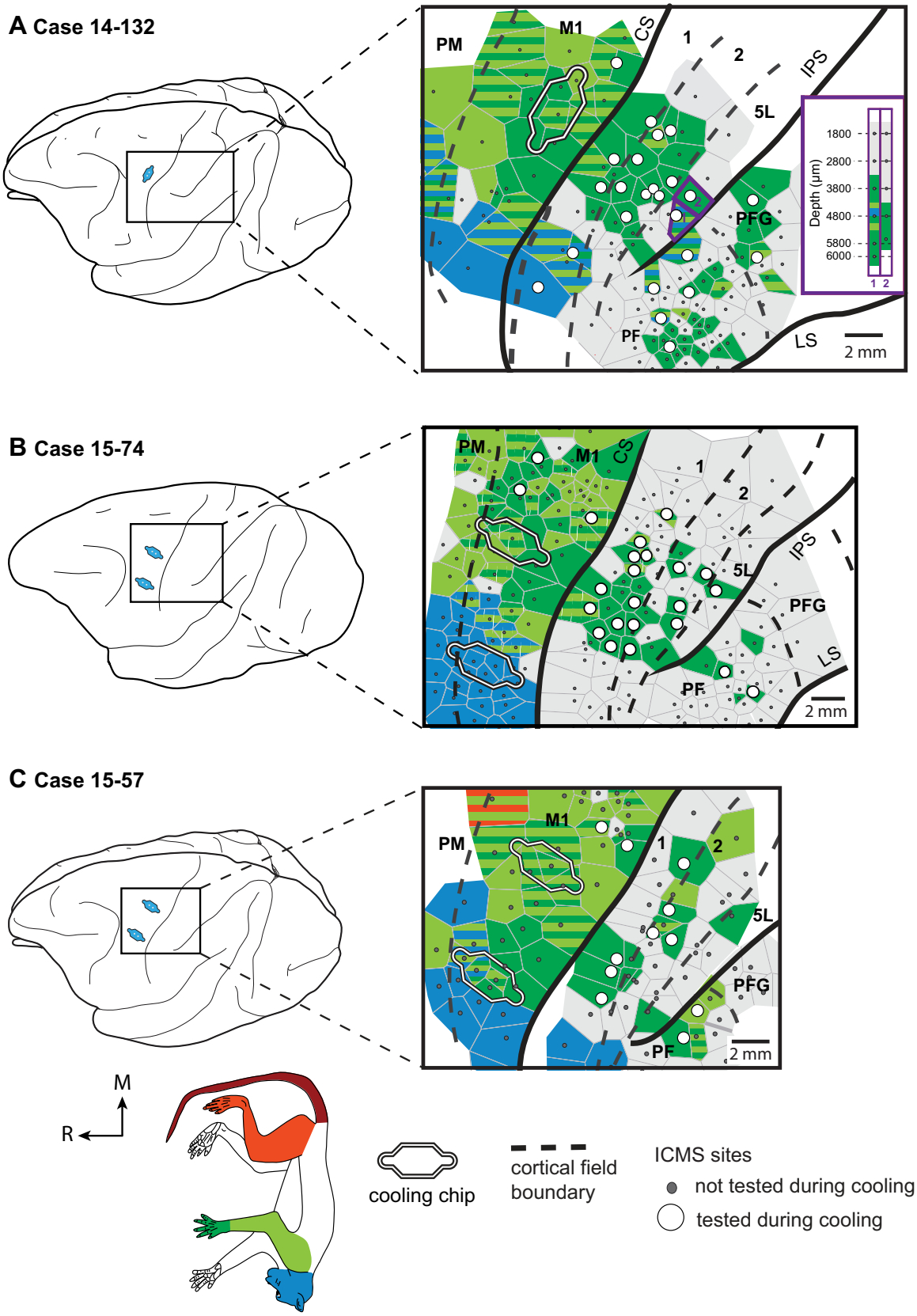

J Neurophysiol • doi:10.1152/jn.00086.2023 • www.jn.org

we placed our chip over areas 2/5 M and used an infrared thermal camera (FLIR A325sc) to examine the extent of cortex that was cooled during activation of the chip. Cortical temperature throughout the six epochs (see Fig. 2 and *Deactivation Protocol* section) was also measured by a microthermocouple (mtc) under the device. Control of the coolant pump was set to maintain the mtc at 10°C. The region cooled to 20°C extended slightly from the edges of the cooling channel (Fig. 2*C*). The extent of cooling shown in Fig. 2*A* is likely an overestimation of the spread of cooling as this is only a measure of surface temperature of the cortex; the spread of cooling at deeper depths is likely much smaller (see Fig. 9 of Ref. 49). The effects of our cooling chips on the activity of neurons in the cooling footprint have been described previously (49), with findings indicating the underlying neurons are robustly inhibited during cooling, but recover to precooling levels of activity/excitability quickly. Because the cooling chips were transparent, we could monitor the integrity of the cortex throughout the experiments and ensure that any deactivation was not due to damage.

Placement of Cooling Chips

Placement of cooling chips on specific motor and premotor movement representations was guided by the initial exploration of motor and premotor cortex using ICMS techniques described above. To ensure a uniform cooling footprint for each chip, we placed chips on relatively flat areas of cortex (e.g., apex of a convexity) and avoided locations at which the cooling footprint would be directly adjacent to sulci or at which part of the chip was not in contact with the cortical surface. Placement relative to architectonic boundaries of cortical fields was later verified histologically (see *Alignment/Reconstruction of Physiological and Anatomical Data*). Each cooling chip was secured to a micromanipulator via a steel wire embedded in a ~1-cm-diam blob of dental acrylic that also encompassed the coolant tubes ~5–10 mm above the cooling chip. Thus, the chips were placed over the forelimb and/or face representations identified by ICMS in M1; in one case, the chip encroached on a small portion of premotor cortex. The flexible silicone coolant tubing allowed the chip to maintain a gentle, consistent pressure on the cortex. The transparent cooling chips (Fig. 1, *D–F*) were photographed relative to the underlying vasculature on the cortical surface before and after the experiment to confirm that chip location did not change.

Deactivation Protocol

After chip implantation, the stimulating electrode was repeatedly lowered into parietal cortex (we also tested a few sites in M1) and if a robust ICMS-evoked movement was present, we collected data on the effects of M1 cooling. We qualitatively judged a robust response as a movement that was consistently evoked by stimulation and that was relatively consistent in amplitude while estimating divergence due to factors such as muscle fatigue, transient neural habituation, or variation in the start position of the limb/facial feature. Our experimental design is illustrated in Fig. 2, bottom panel. Each cooling chip (in the two cases in which two cooling chips were implanted) was activated separately. ICMS movements were compared across six temperature epochs before, during, and after deactivation in M1. For a given site, stimulations across epochs were conducted at the same amplitude of stimulation. The first was the "baseline epoch," during which the temperature under the chip was in a normal range (34–36°C) for exposed cortex without the insulation of the overlying skull. After this, coolant was pumped through the cooling chip until a temperature of 10°C (at the chip-cortex interface) was reached. After 1 min at this target temperature, ICMS was again applied to the same site and evoked movements were recorded ("cooling 1 epoch"). This was repeated 3 and 5 min after target temperature was reached (cooling 3 and 5 epochs, respectively). After this, the pump was turned off and the cortex passively rewarmed. One minute after it reached 34°C, ICMS was tested again (rewarm 1 epoch). This was repeated at 5 min after 34°C was reached (rewarm 5 epoch) when the temperature was typically ~36°C. Throughout all six epochs, the location of the stimulating electrode never changed. In two monkeys, two cooling chips were used sequentially in primary motor cortex, M1. We also ran sham cooling in which we pumped warm ethanol through the cooling devices to rule out the possibility that the effects on evoked movements were due to factors other than cooling (Fig. 9). The timing of these sham tests matched the timing sequence of the epochs described above.

ICMS movements (or the lack of them) were described for each epoch in a written record and video recorded for offline analysis (see below). After all deactivation experiments, fiducial probes were inserted into the brain at selected sites so that stimulation data could be related to histologically processed tissue. See Fig. 3 for final anatomical reconstructions and functional maps.

Histological Procedures

Once ICMS mapping was complete, animals were given a lethal dose of sodium pentobarbital intravenously and perfused transcardially. The brains were removed and postfixed. During horizontal sectioning, block face images were

Figure 3. Location of cooling chips relative to movement representations in M1 for the three cases used in this study (*A–C*). The color code for body part movements is at the bottom left of this figure. *A*: in case 14-132, the cooling chip was placed over the forelimb representation in M1 and 24 sites (white circles) in areas 1, 2, 5L, PF, and PFG were stimulated during cooling. The numbered sites outlined in purple were stimulated at multiple depths within a sulcus (shown in purple outlined *inset*, with depth represented along the *y*-axis). *B*: in case 15-74, one cooling chip was placed over the forelimb representation and one chip was placed over the face representation in M1, and 23 sites were tested in M1, areas 1, 2 5L, and PF. *C*: in case 15-57, one cooling chip was placed over the forelimb representation in M1 while one chip was placed over the forelimb/face representation in M1, and 11 sites were tested in areas 1, 2, and PF. For all cases, the dashed lines represent borders of architectonically defined cortical areas. Solid black lines represent sulci. Large white circles represent electrode penetration sites where ICMS was tested during cooling. Small gray circles represent other electrode penetration sites not tested during cooling. Tiles surrounding circles indicate the body part(s) involved in the ICMS-evoked movement according to the color code at bottom left. Striped tiles indicate movements involving multiple body parts. Gray tiles represent sites where ICMS failed to elicit a movement up to 600 μA. Location of the cooling chip in M1 is outlined. ICMS, intracortical microstimulation.

captured. Serial sections were processed for Nissl staining, which was used to determine borders between cortical fields (see Ref. 29).

Subdivisions of PPC were defined as in previous studies (11, 28). Because we took images of each block face during cutting, we could readily follow the depth and location of electrode penetration sites, including stimulation sites within the central and intraparietal sulcus. We determined that our stimulation sites were located in M1, area 1, area 2, area 5L, PF, and PFG.

Alignment/Reconstruction of Physiological and Anatomical Data

We made a three-dimensional (3-D) reconstruction from the block-face images using the Fiji processing package (51). Locations of borders derived from Nissl-processed sections (for M1, 3a, 3 b, 1, 2, 5L, PF, and PFG) were superimposed on the corresponding block-face images. Fiducial probes located in unstained sections were marked on their corresponding block-face images. Electrode penetrations visible in sections were also highlighted. These 3-D reconstructions were then aligned to images of the surface of the brain using local landmarks such as sulcal locations, as well as electrode and fiducial probe penetration sites. This process allowed us to accurately align histologically determined cortical field boundaries to our microstimulation maps. For additional details of methods, see Ref. 29.

Movement Analysis

All movements were characterized by two independent observers and were recorded during the experiment. These movements were later analyzed and confirmed offline. Movements were qualitatively described during observation, and later quantitatively described in the following two ways.

First, we quantified the amplitude of the movement elicited. To do this, we measured displacement of a tracked body part in the x-y plane from videos. These ICMS-evoked movement displacement profiles were generated by importing the experimental recordings into Tracker analysis and modeling software (http://physlets.org/tracker/) and the position of a specific point arbitrarily chosen at the extremity of a given body part (usually a fingertip or other visually distinctive feature) was monitored and recorded for each frame (1/60 s) relative to ICMS stimulation onset and offset. A scale bar near the location of the moving body part served to calibrate the movement displacements during stimulation (see Figs. 5, 6, and 8 for examples). Representative movements are illustrated by superimposing frames captured just before stimulation initiation (baseline) and at the peak of the movement amplitude (apex) and/or at the conclusion of the stimulation. These frames were imported into Adobe Illustrator where the outline of the body movement was traced. Although previous studies have documented eye movement-related activity, or evoked eye movements via stimulation, in some portions of PPC (52, 53), in the current study we did not stimulate in regions where eye movements have been elicited and did not monitor eye movements.

We next quantified the type of movement elicited. We defined this by noting which forelimb joints or facial features were actuated. The facial features that were observed to move were nostril, lip, tongue, jaw, chin, vibrissae, brow, and eyelid. All of these were included as one "face" category. The limb joints that were observed to move were shoulder, elbow, wrist, and interphalangeal joints of D1, D2, D3, D4 and D5. All of these were included as one "forelimb" category. Neck movements were observed, but excluded from the analyses.

We then characterized interactions between stimulated and cooled sites as potentially homotopic or heterotopic (see Fig. 4 for schematic definition of homotopic and heterotopic). The question we posed with this analysis was whether a given parietal movement representation was affected by deactivating part of motor cortex and, crucially, whether the deactivated representation in M1 was of the same body part as that tested in parietal cortex.

In addition, given the size of the chip footprint (although relatively small), and the mosaic nature of M1 organization, strictly homotopic tests were not possible. Although we could restrict cooling to a large forelimb domain, cooling many different smaller domains (e.g., digit flexion) simultaneously was unavoidable (see Fig. 3). This heterogeneity means that even in homotopic tests some nonanalogous domains may sometimes be cooled along with the analogous domain. Therefore, we classified a test as homotopic if at least one analogous domain was present, whereas tests were heterotopic, if all domains were different. Heterotopic effects likely rely on more complex frontoparietal interactions than do homotopic, so if both types of effects are potential explanations, we assume that the simpler explanation is more likely correct. This definition also provides a stringent test of our hypothesis that macaques show a greater probability of heterotopic effects compared with previously tested species.

Some tests could also result in qualitatively changed movements if additional joints were actuated during cooling that were not present at baseline, or if the direction of a movement changed (e.g., flexion to extension). For example, if a D1 movement was observed during cooling, and only elbow movement was observed before cooling, the movement was considered qualitatively changed. These effects were treated as a separate variable from heterotopicity/homotopicity, though we never observed the addition of a new movement in a nonanalogous body feature to the one that had been actuated at baseline (e.g., no observations of an additional facial movement during cooling or rewarming when stimulating a domain that actuated the arm). A total of nine tests involved qualitative changes, with five tests (at 5 sites) occurring during cooling, and four tests (at 3 additional sites, with one site showing both types) after rewarming. Four tests (at 3 sites) resulted in qualitative changes after rewarming, but without recovery of the baseline movement, and therefore were not included in the analyses.

In the majority of tests, movements returned to baseline within 5 min of rewarming. In total, we found only 14 tests from a total of 101 attempted tests in which movements did not return to baseline, resulting in an ~86% success rate for completed cooling tests. These 14 tests that did not regain excitability during rewarming were excluded from the analysis. The distribution of excluded and retained tests is not significantly different from chance between the areas observed

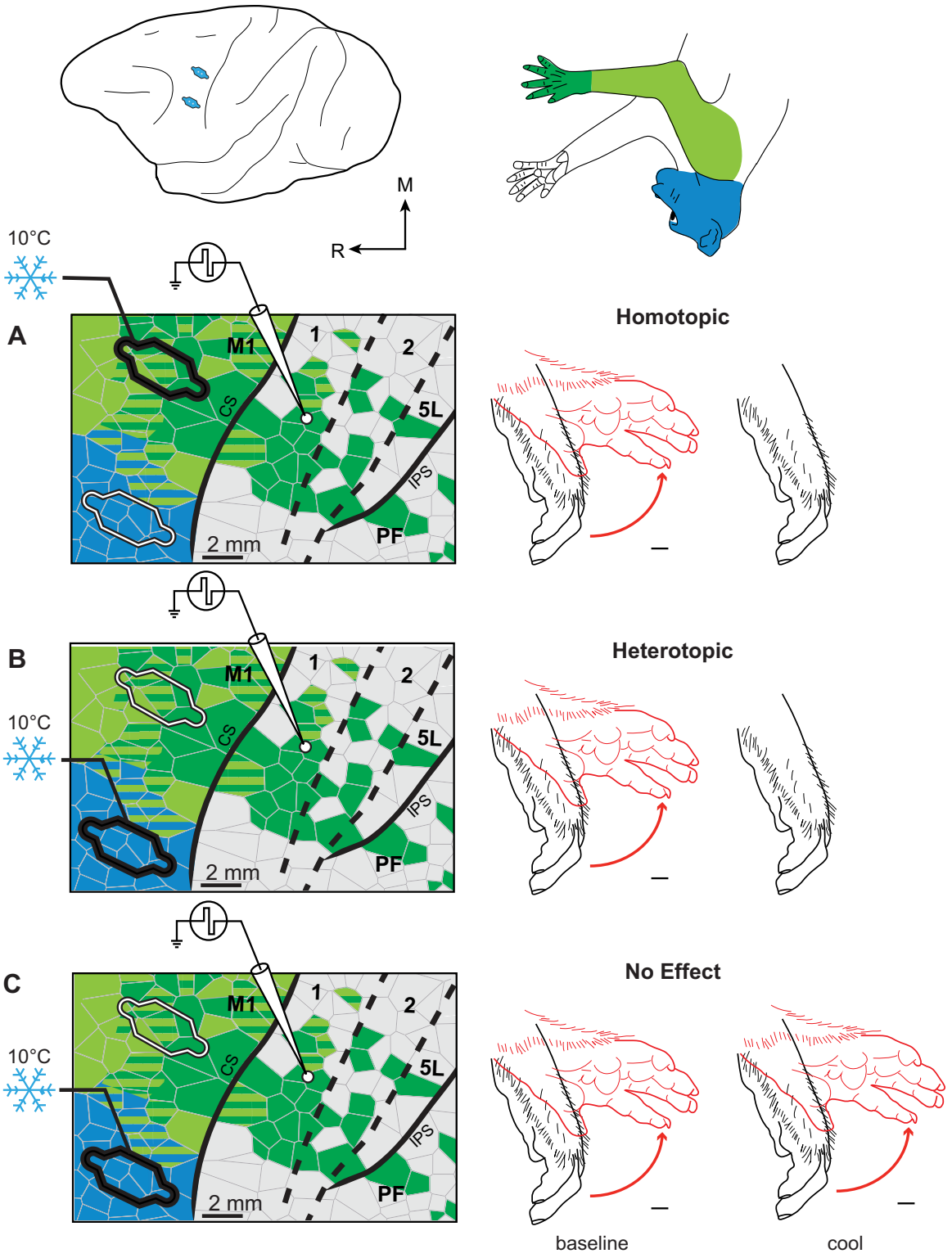

Figure 4. Hypothetical examples of homotopic effects, heterotopic effects, and no effect of cooling M1 for a stimulation site in area 1. The top illustration shows the location of two cooling chips in M1, one in the forelimb representation and one in the face representation, with the body parts color coded at right. *A*: illustrates a homotopic effect in which cooling the forelimb representation in M1 (medial cooling chip, outlined in black) abolishes a forelimb movement evoked by ICMS in area 1. *B*: illustrates a heterotopic effect in which cooling the face representation in M1 abolishes an area 1 ICMS-evoked forelimb movement. *C*: illustrates an alternative outcome to that shown in *B*. Here, there is no effect on an area 1-ICMS-evoked forelimb movement when the face representation in M1 is cooled. For conventions, see previous figures. ICMS, intracortical microstimulation.

[Fisher's Exact test for 2 (excluded, retained) × 6 (area 1, area 2, area 5L, PF, PFG, and M1) contingency table, $P = 0.1$].

We assigned each test an effect category: no effect, reduced amplitude, or abolished. A test was considered to have had a reduced amplitude if movement amplitude was lowered by at least 20% (below 80% of that observed before cooling, which is outside the range of variability of evoked movement), throughout the duration of cooling. A movement was considered abolished if movement amplitude during any cooling epoch was reduced by 90% (less than 10% of that observed before cooling). All other tests were assigned to the no effect category.

Statistical Analyses

All statistical analyses were carried out in MATLAB or Excel using built-in functions. Nonparametric tests were used to assess differences in prevalence of observed effects, due to a low number of observations. Chi-square tests are conventionally used for this type of hypothesis test, but we used Fisher's exact tests (54) because Chi-square tests are unreliable when the expected value in a contingency table cell is under 5, which was incompatible with most analyses in the current study.

A significant P value ($P < 0.05$, or appropriately adjusted via Bonferroni correction for multiple comparisons) was taken as an indicator of an overall asymmetric spatial distribution of electrophysiological effects (a main effect in the statistical sense). Bonferroni corrections were done to correct for familywise error rates. Given that this is an exploratory analysis, we calculated the familywise error rate by the number of tests that we conducted on the same null hypothesis (55). We tested whether the incidence of abolished and/or reduced movement or no effect was different between areas 1 and 2 using two Fisher's exact tests (one contrasting reduced amplitude versus abolished versus no effect, and one contrasting any effect versus no effect), resulting in a corrected α of 0.025. We tested whether the incidence of tests resulting in homotopic versus heterotopic effects was different between areas 1 and 2 using one Fisher's exact test, resulting in no correction. We tested whether any brain areas differed in terms of prevalence of tests excluded from the analyses with one Fisher's exact test, with no correction. We tested whether the lowest amplitude evoked during cooling differed between areas 1 and 2 with one Student's t test, resulting in no correction. Finally, we tested whether the prevalence of movements reduced below a given amplitude differed between areas 1 and 2 using one Kolmogorov–Smirnov test with no correction.

RESULTS

We investigated the effects of deactivating motor cortex via cooling on movements evoked using intracortical microstimulation (ICMS) in anterior and posterior parietal cortical areas. We first describe the location of our cooling chips in the primary motor cortex (M1) and the movement representations that were deactivated during cooling. We then describe the effects of M1 deactivation on movements evoked by ICMS in anterior parietal cortical fields (areas 1 and 2) and posterior parietal cortical fields (PPC, areas 5L, PF, and PFG). We distinguish three major types of effects: movements abolished, movements reduced, and no effect on movement. We also noted if a movement changed qualitatively. We assessed these effects on movement representations that were analogous to those that were deactivated in M1 (homotopic) as well as on representations that were different than those deactivated in M1 (heterotopic).

Placement of Cooling Chips in M1

The placement of cooling chips over specific movement domains was guided by ICMS mapping of M1. Cortical field boundaries were later verified from Nissl-stained histological sections, as previously reported (29). All chips were placed over M1, with only the corner of two chips slightly extending over premotor cortex (PM, Fig. 3). As described in MATERIALS AND METHODS, elicited movements were defined by the joints that were actuated during stimulation, and ultimately categorized simply as "forelimb" or "face" based on which body part was actuated.

Cortical maps for each animal are illustrated in Fig. 3, which shows cooling chip placement (white outlines, representing the physical footprint of the coolant channel) along with ICMS movement maps, color-coded for each body part involved in the movement. The subset of sites tested during cooling is also shown (white circles). As can be seen from Fig. 3, in all cases, chips placed in M1 medially cooled forelimb representations (green). The chip placed in M1 laterally cooled face representations (blue) in cases 15–74 (Fig. 3*B*), or forelimb and face domains in cases 15–57 (Fig. 3*C*), and in cases 14–132 (Fig. 3*A*) no lateral chip was used. As in previous studies (5), we defined movement domains based simply on whether the movement occurred in the forelimb, or the face, or both.

Across all three animals, we analyzed 58 sites with 87 tests. There is not a 1:1 correspondence between the number of tests and number of sites because 29 sites were tested with only one chip, leaving 29 that were tested with two chips. In total, we analyzed 38 anterior parietal sites with 58 tests, 14 posterior parietal sites with 18 tests, and 6 M1 sites with 11 tests. To confirm the consistency of effects, sites underwent multiple cooling tests with a given chip, but these subsequent tests were not included in this analysis. Following cooling, 83% of all evoked movements recovered to well above the 10% criterion for abolition. The mean level of recovery was 80% (SD 27%). Of the tests considered recovered, 68% recovered to above 80%, 7% recovered between 60–80%, 15% recovered between 40–60%, and 10% recovered between 15–40%.

Homotopic and Heterotopic Cooling Effects

Because we are investigating the evolutionary trend of increasing "interconnectedness" in the primate motor control network, we were particularly interested in different types of functional interactions between movement representations in motor cortex and parietal cortex. The first type of interaction, termed homotopic, was between movement representations involving the same body part, (for example: M1 elbow flexion and area 1 elbow extension). The second type of interaction, termed heterotopic, was between movement representations involving different body parts, (for example: M1 face and area 1 elbow flexion). An illustration of

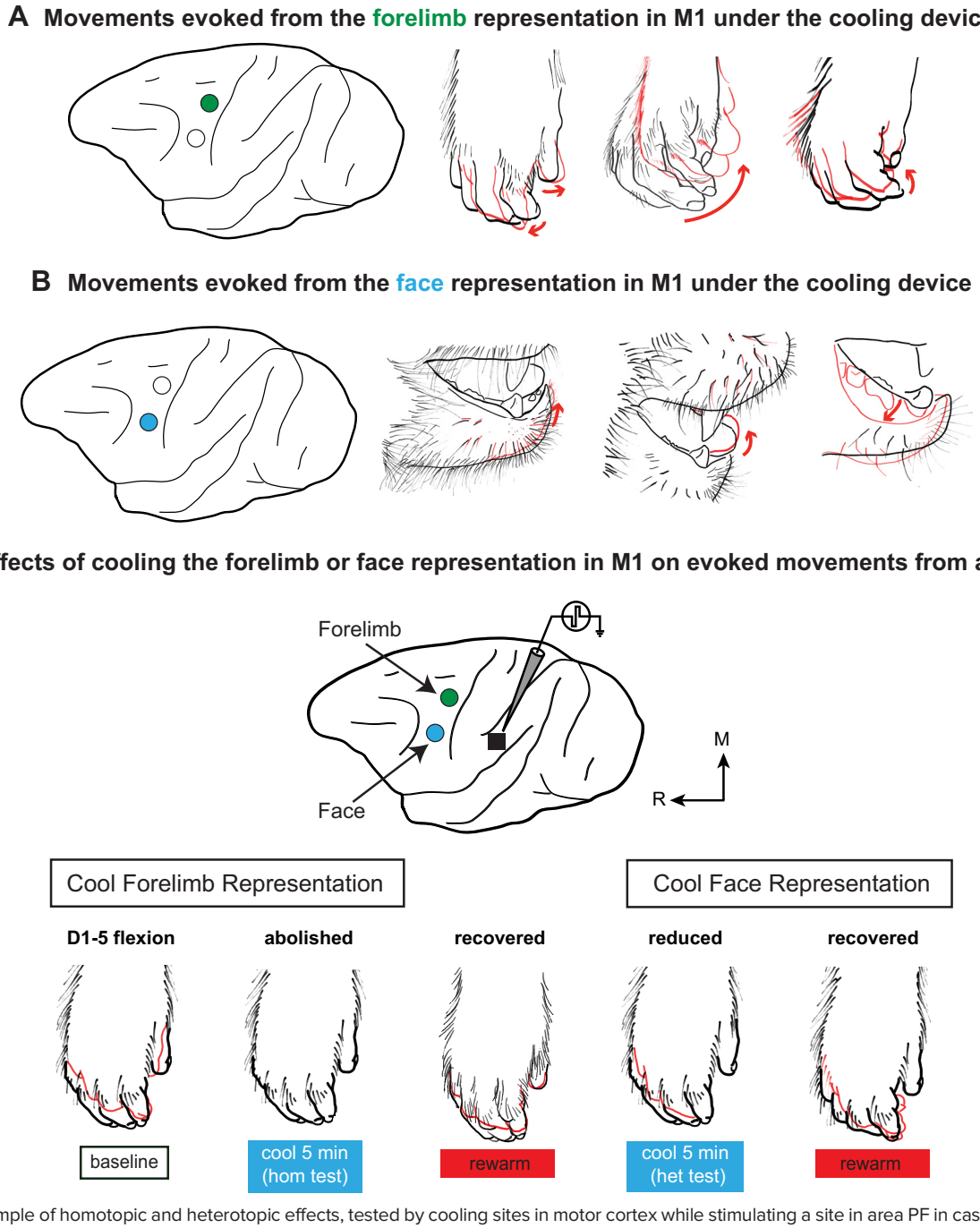

Figure 5. Example of homotopic and heterotopic effects, tested by cooling sites in motor cortex while stimulating a site in area PF in case 15-74. *A*: representative movements evoked from three sites in M1 under the medial cooling chip (out of 10 stimulation sites under and within 2 mm of this cooling chip). *Left*: location of ICMS stimulation site and the cooling chip placement (green circle), shown on a schematic of the macaque brain. Stimulation at all sites actuated the hand or portions of the forelimb (not shown). *Right*: black traces of video frames show baseline posture just before ICMS, and red traces show apex posture, where the body part was maximally displaced by ICMS. Red arrows show the direction of movement and approximate path of the feature highlighted. *B*: representative movements evoked from stimulation of three sites in M1 under the lateral cooling chip (out of 20 under and within 2 mm of this cooling chip). *Left*: location of ICMS stimulation sites and the cooling chip placement in M1 (blue circle). Other conventions as in *A*. *C*: sequential cooling and rewarming of two chips in M1 while stimulating one site in area PF. The brain outline at the top illustrates the location of the cooling chips in M1 and the location of the stimulation site in PF (black square). Lower illustrations show forelimb pose at rest (black) and at the apex of evoked movement (red). The first column illustrates flexion of the digits when area PF is stimulated (baseline, with no cooling/rewarming). This movement was similar to those evoked from sites under the medial chip, but dissimilar to sites under the lateral cooling chip (over the face representation). The second column shows abolished movement when forelimb (medial) M1 sites are cooled, demonstrating a homotopic effect. The third column shows that the movement is recovered when the area in M1 is allowed to rewarm. The fourth column shows that during cooling of face representations, no movement of digits 1 and 2 could be evoked and only small movements of digits 3–5 were observed, indicating a heterotopic effect. The fifth column shows recovered movement after rewarming. ICMS, intracortical microstimulation.

these three types of effects is shown in Fig. 4. A case in which these types of effects could be determined by activating different chips in the same animal for the same stimulation site is presented in Fig. 5, showing stimulation of a site in area PF, in cases 15–74. Here, cooling the forelimb representation in M1 resulted in a homotopic effect, indicated by the fact that movement evoked from representations of the hand was abolished. Cooling the face representation in M1 also resulted in a heterotopic effect at this same site. Figure 6 additionally shows two examples of heterotopic effects evoked from two area 1 sites in this same animal (cases 15–74). We considered any change (reduced, abolished, or qualitatively changed ICMS-evoked movement) to be evidence of an effect of cooling, though we never observed qualitative changes without reduction in movement amplitude. Some of the interactions described above may reflect direct anatomical connections, but given the diversity of movement representations cooled in M1, the functional relationship we observed likely arose from multiple anatomical connections throughout a large and distributed motor control network. Although the circuitry of this network is beyond the scope of this investigation, this study lays the groundwork for future studies that interrogate the mechanisms behind the functional interactions investigated here.

Qualitatively Changed Cooling Effects

We sometimes evoked new movements during cooling that were not observed during baseline, including changing direction of a movement or adding new parts/joints to the movement. These qualitative changes occurred during cooling, and sometimes persisted into the rewarming epoch, or sometimes occurred only during rewarming.

For an example of a qualitatively changed movement see Fig. 6*B*. Baseline stimulation of this site evoked a complex forelimb movement composed of D1 adduction and retroflexion, D2 abduction, D2-5 flexion, and slight wrist extension. Cooling the lateral chip, over the lip representation in M1, resulted in a loss of all movements observed at baseline,

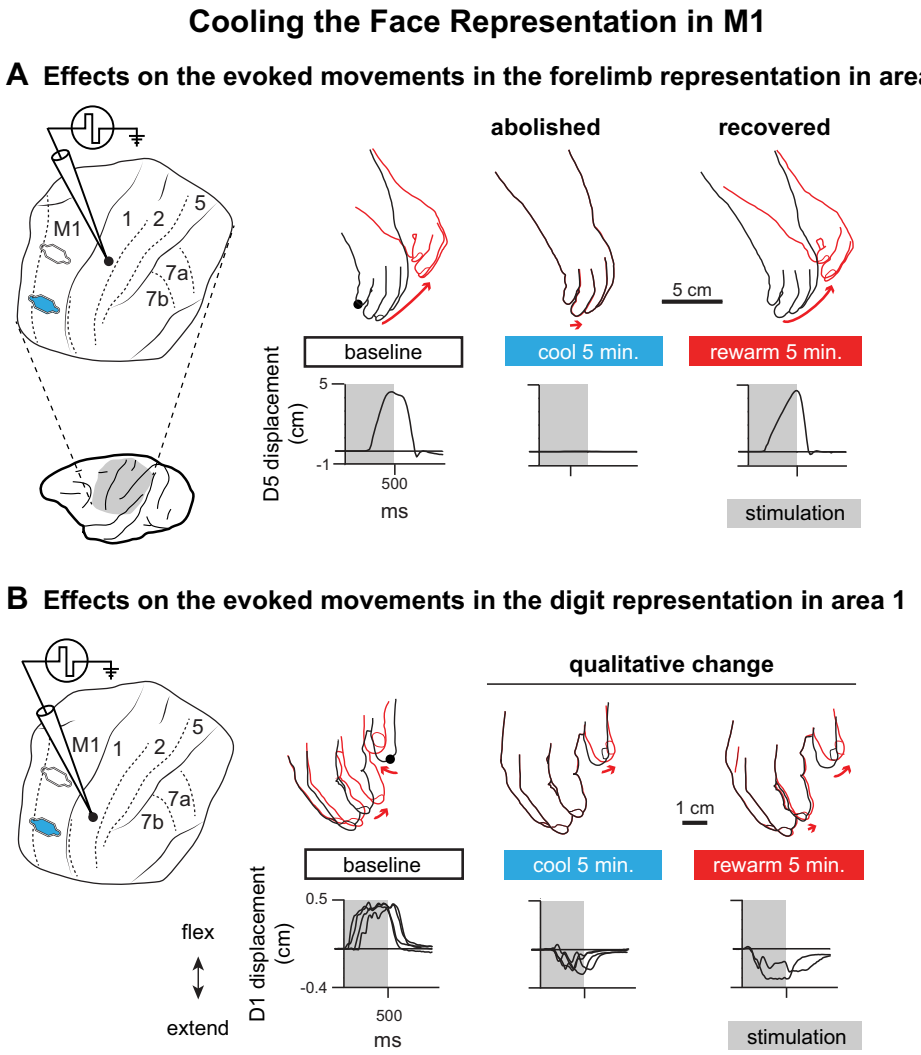

Figure 6. Movements evoked by ICMS in two locations in area 1 in case 15-74, during cooling/warming of the face representation of M1. These reveal two types of heterotopic effects: abolition of the movement (*A*) and abolition of baseline movement with the addition of a qualitatively changed movement during stimulation (*B*). In both *A* and *B*, the outline of the hand was traced from video frames just before (black; baseline) and during (red) ICMS. The plots show displacement of the digit tip (labeled above each plot with a black circle in the baseline tracing) during 500 ms stimulation (gray shading) and passive relaxation (no shading). Plot *B* shows superimposed data from four stimulation trials. ICMS, intracortical microstimulation.

J Neurophysiol • doi:10.1152/jn.00086.2023 • www.jn.org

but there was an addition of a small D1 extension and abduction. This additional movement is particularly notable for the sign change of movement direction: from flexion to extension and adduction to abduction. Qualitative changes such as these were rare, with only 9 out of 86 tests analyzed evoking a qualitatively different movement at any point. Five of these changed movements occurred during cooling epochs, whereas four occurred during rewarming. Four additional tests that did not recover the baseline movement evoked a qualitatively changed movement after rewarming, though these were not included in analyses.

Effects of Cooling M1 on Anterior Parietal Fields Area 1 and Area 2

The majority of sites we tested were in areas 1 and 2 (see Table 1). Compared with area 2, area 1 had fewer tests that resulted in abolished movements [34% in area 1 vs. 74% in area 2, Fisher's exact test for 2 (abolished and not abolished) $\times$ 2 (area1 and area2) contingency table, $P = 0.007$]. The distribution of amplitudes also differed between the two areas, with tests in area 2 skewing toward the low end of values. Tests in area 1 also skew toward the low end of the distribution but are more evenly distributed than area 2 (see Fig. 7*A*). Figure 7*B* shows a cumulative distribution function for each area tested, highlighting the fact that the distribution for area 2 shows consistently lower values of retained movement compared with the other areas. However, this difference is not statistically significant [Kolmogorov–Smirnov test, $D(35, 23) = 0.17$, $P = 0.5$].

Most tests in either area resulted in a monotonic decrease in movement amplitude with increased cooling duration, meaning that movement evoked during cooling at 1 min, 3 min, and 5 min became progressively smaller. However, the effects of cooling M1 on area 1 tended to be more variable than area 2, with four tests showing some recovery at 3 min of cooling (before reducing in amplitude again at 5 min), and three tests showing some recovery at 5 min compared with 3. Only one test in area 2 showed a nonmonotonic pattern. This difference is commented on as a qualitative observation and is not statistically significant (it was not examined, due to the low number of tests).

Cooling M1 had hetero- and homotopic effects on both areas 1 and 2, and there was no significant difference in the prevalence of either type of effect within or between areas [Fisher's exact test for 2 (homotopic and heterotopic) $\times$ 2 (area1 and area2) contingency table, $P = 0.24$, and see Table 1].

In all, we observed a trend in which neurons in area 1 were less susceptible to M1 cooling compared with neurons in area 2. This lower susceptibility of area 1 was indicated by a higher prevalence of *1*) tests that resulted in no effect, *2*) tests that showed a nonmonotonic decrease in movement amplitude as cooling progressed, and *3*) tests that retained a higher movement amplitude.

Effects of Cooling M1 on Posterior Parietal Areas 5L, PF, and PFG

The effects of cooling M1 on PPC areas were qualitatively similar to those observed in area 2. See Figs. 5 and 8 for examples of tests in PPC (areas PF and PFG). Overall, all 18 tests at 14 sites resulted in abolished or reduced amplitude of evoked movements during M1 cooling (See Table 1). Figure 8 shows an example site in area PFG, in which an evoked movement was completely abolished during the first 1-min-long cooling epoch. At this site, forelimb movements were evoked at baseline, abolished during cooling of an analogous representation in M1, and then recovered with rewarming. Both sites tested in area PFG showed homotopic effects; no heterotopic tests were attempted in this area. Both homotopic and heterotopic effects were observed across areas in PPC, but we do not speculate on the relative prevalence of either, due to the small sample for each individual area of PPC.

The Intrinsic Effects of Cooling M1

We examined the effects of cooling M1 at other sites in M1 or adjacent to the cooling chip. Nine of 11 tests at 6 sites (82%) had reduced amplitude or abolished movement when M1 was cooled, making M1 proportionately the least affected area tested. Most of these affected sites were homotopic, with only 1 of 3 heterotopic tests resulting in an effect, though again the small number of observations limits statistical power.

Table 1. *Effects of cooling M1 on each cortical area stimulated*

Sites Attempted					Tests Attempted		
	Total Sites	Nonrecovered	Analyzed		Total Tests	Nonrecovered	Analyzed
Total	63	9	58	Total	101	14	87

Sites analyzed							
	Area 1	Area 2	Area 5L	Area PF	Area PFG	M1	Totals
Total	21	17	3	9	2	6	58

Tests analyzed							
	Area 1	Area 2	Area 5L	Area PF	Area PFG	M1	
Total	35	23	4	12	2	11	87
Tests resulting in no effect	4	0	0	0	0	2	6
Reduced amplitude of movement	19	6	1	4	0	5	35
Abolished movement	12	17	3	8	2	4	46
Homotopic effects/tests	19/22	18/18	3/3	8/8	2/2	8/8	58/61
Heterotopic effects/ tests	12/13	5/5	1/1	4/4	0/0	1/3	23/26

For an explanation of homotopic and heterotopic, see main text. There is not a 1:1 correspondence between the number of tests and number of sites because 28 sites were examined both during medial and lateral chip cooling while 30 sites were only tested once, with either medial or lateral chip cooling, but not both.

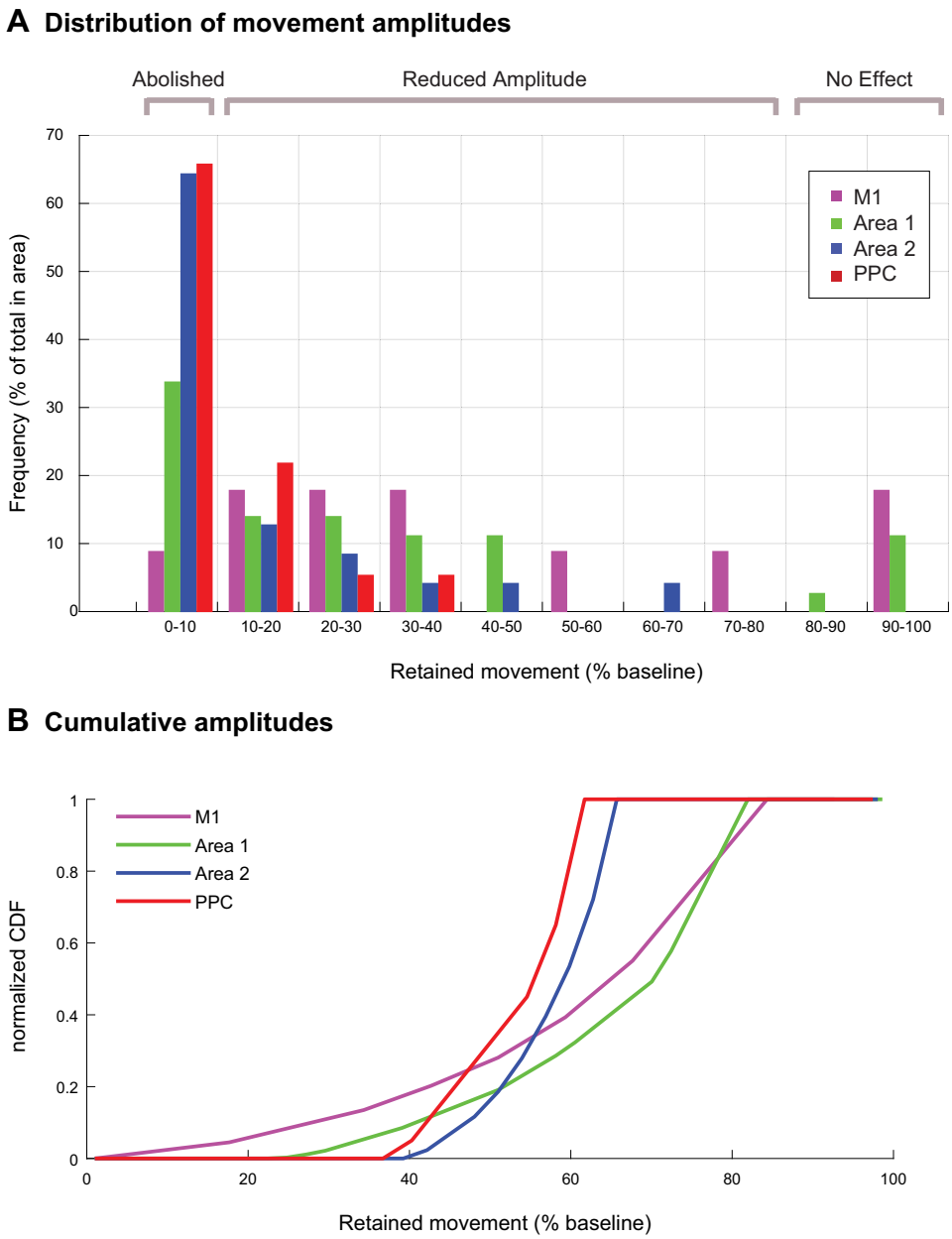

Figure 7. Movement amplitudes during cooling tests for sites in M1 (purple), area 1 (green), area 2 (blue), and PPC (red). *A*: distribution of movement amplitudes exhibited during cooling tests, shown as a percent of tests in each area that were inhibited to a given percent of baseline amplitude. Area 2 shows a trend toward a higher prevalence of abolished tests, few reduced tests, and no tests resulting in no effect. In contrast, area 1 had fewer tests with abolished movement, more tests resulting in reduced amplitudes, and some tests with no effect, indicating this area may be less sensitive to M1 cooling than area 2. Qualitatively, the pattern of effects for sites in PPC resemble that of area 2, while sites in M1 resemble that of area 1. *B*: cumulative distribution functions for each area. The number of tests reduced below a given percent of baseline is not significantly lower for area 2 than for area 1 [Kolmogorov–Smirnov test, $D(35, 23) = 0.17$ $P = 0.5$], though the same potential qualitative differences for area 1/M1 and area 2/PPC are highlighted by the differences in slope. Areas of PPC were pooled for visual representation, but statistical tests were not performed on these data or data from M1.

Consistency of Effects

To rule out variability in the plane of anesthesia as the source of changes in ICMS-evoked movements, we conducted sham cooling (Fig. 8). This site shown in Fig. 8 in PFG first shows abolition of movement with true cooling of M1, followed by complete recovery to baseline movement. We then conducted the same testing procedures except that we ran warm rather than cooled ethanol through the chip. This sham cooling had no effect on the movement throughout the test. Seven sham cooling tests were performed, only one of which coincided with a moderate reduction of movement amplitude, and moderately variable movement amplitudes were also observed from this site during the baseline epoch. We also conducted control tests in which sites, where an effect of cooling was

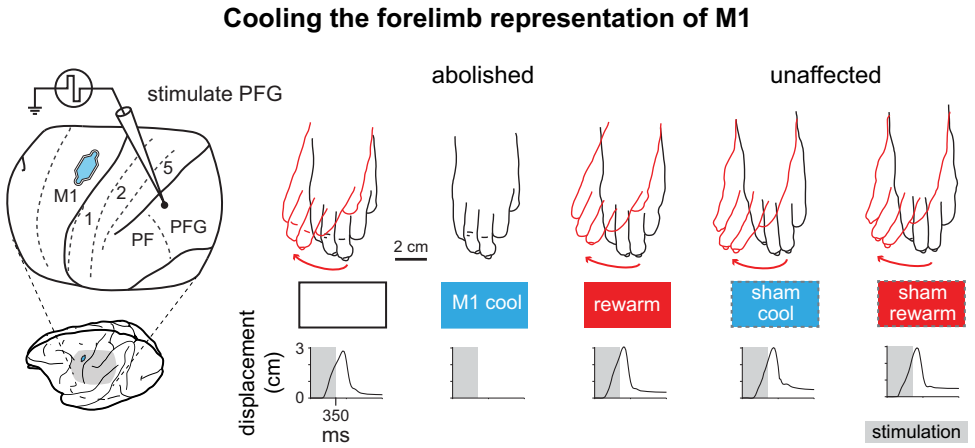

Figure 8. Example of homotopic effects and sham cooling during ICMS in area PFG of case 14-132 with cooling/warming of the forelimb region of M1. Movement evoked at baseline (wrist ulnar deviation) is abolished during cooling, recovered after rewarming, and remains unchanged during sham cooling and rewarming. The relative placement of the ICMS site and cooling chip is shown in the left illustrations. Conventions as in Fig. 6. ICMS, intracortical microstimulation.

observed, were then cooled again after half an hour or more. Four sites were retested in this manner, with all but one resulting in very similar or identical effects during the second round of cooling and rewarming.

Finally, we tested whether a reduction or abolition of movement was attributable to direct deactivation of that site due to spread of cooling from the activated chip, by stimulating sites near the chip during cooling. Specifically, we found sites close to the cooling chips were not more affected by cooling than sites far from the chip. For example, Fig. 9 shows two stimulation sites in M1 (close to the chip), two at which evoked movements were unaffected, and one at which evoked movements were moderately affected, whereas evoked movement at many of the sites far from the chip were strongly affected by cooling. Overall, these data indicate that spread of cooling around the chip did not contribute to these results. Taken together, our sham cooling, retesting of sites, and testing at different distances from the cooling chip indicate that anesthetic level and spread of cooling away from the chip did not account for the effects of cooling M1 on anterior and posterior parietal cortical areas.

DISCUSSION

In the current investigation, we found that cortical areas were differentially impacted when M1 was inactivated using reversible cooling techniques. One notable result is that area 1 had the least sensitivity to M1 cooling: it had the most tests with no effect and had the fewest tests in which movement was abolished, which contrasts with the higher sensitivity found in area 2. A second important result is that cooling M1 affected both similar movement domains (homotopic) as well as dissimilar movement domains (heterotopic) in roughly similar proportions. Finally, we observed that areas in PPC may also be sensitive to cooling M1. For example, in area 5L and PFG, respectively, three of four tests (at 3 sites) and two of two tests (at 2 sites) resulted in abolished movements, and in area PF 8 of 12 tests (~67%, at 9 sites) resulted in the abolition of evoked movement, with four of 12 tests (33%) resulting in movement reduction.

These results are significant for several reasons. First, examining the functional relationship between motor cortex and areas in parietal cortex in macaques is important because, like humans, macaques have distributed control of the limbs across a wide swath of cortex. Moreover, their hand morphology and use closely resembles that of humans, in contrast to other primate models that have been used in similar studies. Thus, data in macaques can be more readily extrapolated to humans. Second, we show here that M1 in macaque monkeys has equally strong heterotopic and homotopic interactions with parietal areas, which stands in contrast to data from other species in which heterotopic interactions are far less prevalent. This higher prevalence suggests that in Old World monkeys (and likely humans), the cortical circuitry to control movement has become more complex along with the expansion of areas involved in motor control of the forelimbs. Third, this is the first study to test the functional relationship between M1 and somatosensory areas 1 and 2 in primates by cooling cortical areas, a technique that provides more precise temporal resolution than chemical mechanisms for manipulating excitation/inhibition, such as muscimol. Given the more limited effects of M1 inactivation on area 1 compared with area 2 and PPC, it is possible that these areas participate in separate parallel networks that are involved in motor control. If so, this could have a profound impact on rehabilitation and recovery following injuries to M1.

Previous experiments in New World monkeys (6) and galagos (5, 6) that used inactivation techniques to examine the functional relationship between M1 and PPC (likely portions of area 5) found that deactivating M1 abolished or greatly reduced the amplitude of evoked movements in PPC. In macaques, we demonstrate a similar result. However, an important difference between macaques and prosimians or New World monkeys is that inactivation of macaque M1 affected not only similar movement representations to those inactivated in M1 but also dissimilar movement representations. This increase in heterotopic interactions in macaques aligns with the known increase in anatomical connectivity between frontal and posterior parietal cortex and the increase in complexity of motor control in macaques (18, 29, 56), particularly relative to galagos (with no opposable thumb and less manual dexterity). This finding may seem at odds with previous studies in which long-range connections between cortical areas tend to be largely restricted to similar body part representations (e.g., forelimb vs. face) (14, 15, 18, 57). However, we stress that our results do not necessarily

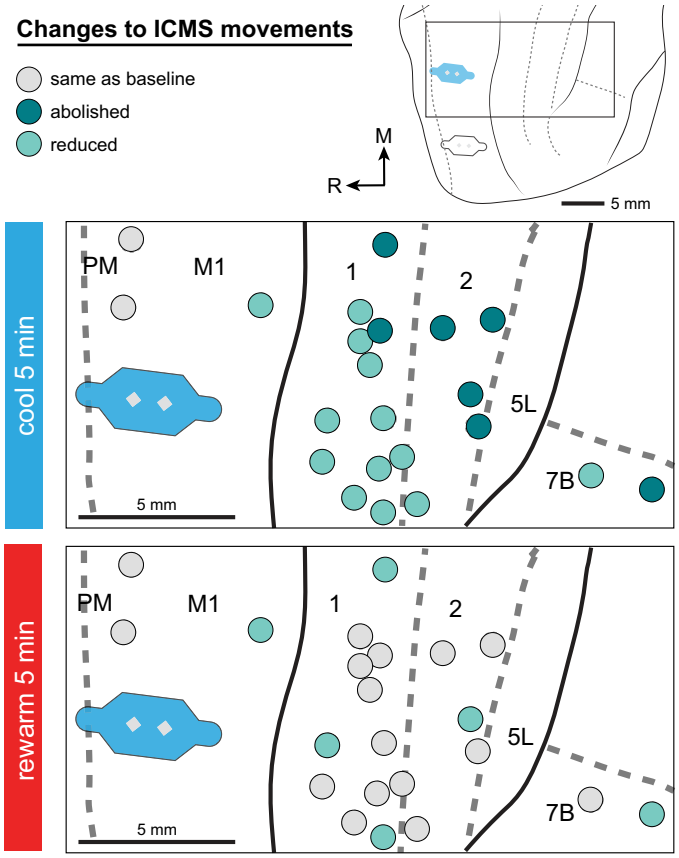

Figure 9. Spatial distribution of changes to ICMS evoked movements during and after cooling the medial chip for case 15-74, showing that cooling M1 caused widespread abolition or reduction in the magnitude of movements evoked from ICMS sites shown in parietal and posterior parietal cortex, but spared 2 of 3 adjacent M1 sites. *Top left*: color key showing status of evoked movement during cooling or rewarming epoch. *Top right*: brain schematic showing cortical location of the boxed region in subsequent panels. *Middle*: the effect at a given site of cooling M1, showing the largest magnitude decrease across all cooling epochs. *Bottom*: effects remaining 5 min after rewarming. Note that ICMS sites nearer to the site of cooling are not more likely to be affected (e.g., see gray circle directly above chip), confirming that cooling's effect is not due to direct cooling deactivation of ICMS sites. ICMS, intracortical microstimulation.

reflect direct anatomical connections between different cortical fields but could also be due to subcortical connections from the transthalamic pathway (cortico-thalamo-cortical (58) or basal ganglia (59) among others).

In a previous study, we proposed that the relative size and number of cortical fields in parietal cortex in different species correlates with homotopic and heterotopic effect prevalence (5). Specifically, we predicted that frontoparietal interactions would become more complex as PPC expands, with both homotopic and heterotopic interactions increasingly likely. Taken together with results in tree shrews (32), galagos (5), and New World monkeys (6, 60), our study and a related study in macaques (29) supports the position that, within all nonhuman mammals investigated thus far, the size of PPC may correlate with complexity of motor control. Essentially, we show that macaques, with the relatively largest PPC of mammals investigated, the most mosaic and widely distributed representations of multijoint movements, and the greatest manual dexterity, also have the highest probability of heterotopic interactions (Fig. 10), an effect which may reflect increased complexity of motor control networks. These

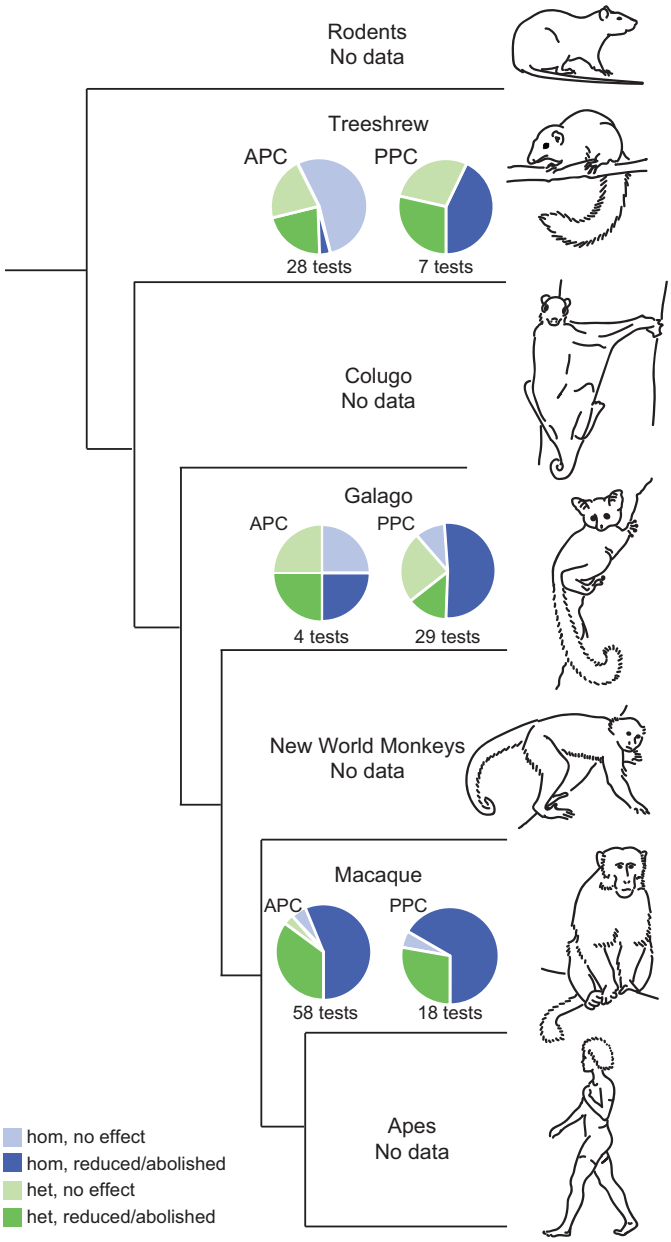

Figure 10. The prevalence of functional interactions (darker shades of blue or green in pie chart) between parietal and frontal areas increases among euarchontoglires as we sample species that are more specialized for manual dexterity (e.g. macaques). Specialized adaptations for manual dexterity are most evident in the primate lineage, followed by colugos and tree shrews, their closest living relatives, and then the more distantly related rodents (rats) and lagomorphs. Results of tests in APC and PPC are shown as pie charts. Blue represents homotopic tests, whereas green represents heterotopic. Darker colors represent reduced amplitude or abolished movement while lighter shades represent attempted tests in which movement was unaffected. Functional data for tree shrews from Ref. 61. Functional data for galagos from Ref. 5. Functional data for macaques from the current study. Note that APC data for tree shrews were recorded predominantly from area 3 b, whereas data for other species were predominantly taken from areas 1 and 2.

J Neurophysiol • doi:10.1152/jn.00086.2023 • www.jn.org

functional differences in macaques contribute to more numerous and varied muscle synergies across major muscle groups, supporting the expansion of the primate manual behavioral repertoire observed in Old World monkeys.

As noted above, the functional interactions between M1 and APC (e.g., areas 3 b, 1, and 2) using reversible inactivation techniques have not been examined in any primate, although preliminary results have been reported for tree shrews (61). While our results for area 2 were similar to those noted for posterior parietal areas (e.g., inactivation of M1 abolished/greatly reduced evoked movements in area 2), our results for area 1 were markedly different, with M1 having a weaker functional interaction with area 1. Area 1 processes cutaneous inputs, is involved in texture discrimination (see Ref. 62 for review), and receives dense inputs from somatosensory areas of the cortex and nuclei of the thalamus as well as from several posterior parietal areas (e.g., 5L and 5M) (12, 14, 15, 63–65). The fact that area 1 was the least susceptible to M1 cooling may be due, in part, to its limited anatomical connections with M1. Unlike posterior parietal areas, the connections between M1 and area 1 are only sparse to moderate in New World monkeys (3, 66, 67) and extremely sparse in macaque monkeys (18). Furthermore, like areas in PPC, area 1 has direct corticospinal connections (10, 37). However, as noted above, it is likely that the functional relationship that we observe may also involve subcortical connections.

What is under investigation here is not the anatomical mechanisms underlying the effects we observe in area 1, but the actual role of somatosensory areas in motor control, and the potential independent nature of their relationship with M1. Intracortical microstimulation studies in a variety of mammals including rats, tree shrews, bats, capuchin monkeys, and macaques (29, 31, 33–35) indicate that somatosensory cortex is involved in motor control, in that movements can be evoked in cortical fields considered to be part of the somatosensory cortex (e.g., S1/3b, area 1 and area 2). Although data are limited, studies in tree shrews demonstrate that evoked movements of APC (S1) are relatively unaffected during M1 inactivation, indicating potential independence of these two cortical movement control networks (61).

Experimental studies of stroke in rats support the existence of two at least somewhat dissociable movement systems involving M1 and S1. Movement deficits resulting from experimentally induced strokes depend on not only the size of the lesion but also the location of the lesion (68). Lesions that include S1 (specifically, areas that architectonically correlate with the forelimb and hindlimb representation of S1, which are also traditionally considered the caudal forelimb area of M1; see Ref. 33), result in different movement deficits compared with lesions in motor cortex (68). These qualitative differences indicate that movements initiated in S1 and M1 can be functionally dissociated.

In all, data from different species, using a variety of experimental techniques, suggest that a parallel system involved in motor control evolved in mammals, and its dependence on motor cortex has been altered in different lineages. The current study expands this data to include a catarrhine primate, the macaque, supporting the existence, and increased complexity, of such parallel networks in a lineage yet one step closer to our own.

DATA AVAILABILITY

Data will be made available upon reasonable request.

ACKNOWLEDGMENTS

We thank Arnold Chen, Scott Simon, Jeff Padberg, Deepa Ramamurthy, and Ian Strieter for their help.

GRANTS

This work was supported by Eunice Kennedy Shriver National Institute of Child Health and Human Development (NICHD) Grant F32 HD103481-01A1 (to C. S. Bresee), by National Institute of Neurological Disorders and Stroke Grant R01 NS035103 (to L. A. Krubitzer), and by James S. McDonnell Foundation Grant 220020516-0 (to L. A. Krubitzer).

DISCLOSURES

No conflicts of interest, financial or otherwise, are declared by the authors.

AUTHOR CONTRIBUTIONS

D.F.C., A.B.G., M.K.L.B., and L.A.K. conceived and designed research; D.F.C., A.B.G., M.K.L.B., C.R.P., and L.A.K. performed experiments; C.S.B. and D.F.C. analyzed data; C.S.B., D.F.C., and L.A.K. interpreted results of experiments; C.S.B., D.F.C., and L.A.K. prepared figures; C.S.B. drafted manuscript; C.S.B., D.F.C., M.K.L.B., and L.A.K. edited and revised manuscript; C.S.B., D.F.C., M.K.L.B., C.R.P., and L.A.K. approved final version of manuscript.

REFERENCES

1. **Goldring AB**, **Krubitzer LA.** Evolution of parietal cortex in mammals: from manipulation to tool use. In: *Evolution of Nervous Systems* (2nd ed.), edited by Krubitzer L, Kaas JH. London: Elsevier, 2017 vol. 3, chapt. 14, p. 259–286. doi:10.1016/B978-0-12-804042-3.00086-5.
2. **Strick P**, **Dum R**, **Rathelot J.** The cortical motor areas and the emergence of motor skills: a neuroanatomical perspective. *Annu Rev Neurosci* 44: 425–447, 2021. doi:10.1146/annurev-neuro-070918-050216.
3. **Gharbawie OA**, **Stepniewska I**, **Kaas JH.** Cortical connections of functional zones in posterior parietal cortex and frontal cortex motor regions in new world monkeys. *Cereb Cortex* 21: 1981–2002, 2011. doi:10.1093/cercor/bhq260.
4. **Wang Q**, **Liao C-C**, **Stepniewska I**, **Gabi M**, **Kaas J.** Cortical connections of the functional domain for climbing or running in posterior parietal cortex of galagos. *J Comp Neurol* 529: 2789–2812, 2021. doi:10.1002/cne.25123.
5. **Cooke DF**, **Stepniewska I**, **Miller DJ**, **Kaas JH**, **Krubitzer L.** Reversible deactivation of motor cortex reveals functional connectivity with posterior parietal cortex in the prosimian calago (*Otolemur garnettii*). *J Neurosci* 35: 14406–14422, 2015. doi:10.1523/JNEUROSCI.1468-15.2015.
6. **Stepniewska I**, **Gharbawie O**, **Burish M**, **Kaas J.** Effects of muscimol inactivations of functional domains in motor, premotor, and posterior parietal cortex on complex movements evoked by electrical stimulation. *J Neurophysiol* 111: 1100–1119, 2014. doi:10.1152/jn.00491.2013.
7. **Averbeck BB**, **Battaglia-Mayer A**, **Guglielmo C**, **Caminiti R.** Statistical analysis of parieto-frontal cognitive-motor networks. *J Neurophysiol* 102: 1911–1920, 2009. doi:10.1152/jn.00519.2009.
8. **Bakola S**, **Passarelli L**, **Gamberini M**, **Fattori P**, **Galletti C.** Cortical connectivity suggests a role in limb coordination for macaque area PE of the superior parietal cortex. *J Neurosci* 33: 6648–6658, 2013. doi:10.1523/JNEUROSCI.4685-12.2013.
9. **Caminiti R**, **Girard G**, **Battaglia-Mayer A**, **Borra E**, **Schito A**, **Innocenti G**, **Luppino G.** The complex hodological architecture of the macaque dorsal intraparietal areas as emerging from neural tracers and DW-MRI tractography. *eNeuro* 8: ENEURO.0102-21.2021, 2021. doi:10.1523/ENEURO.0102-21.2021.

10. **Galea M**, **Darian-Smith I.** Multiple corticospinal neuron populations in the macaque monkey are specified by their unique cortical origins, spinal terminations, and connections. *Cereb Cortex* 4: 166–194, 1994. doi:10.1093/cercor/4.2.166.
11. **Gregoriou G**, **Borra E**, **Matelli M**, **Luppino G.** Architectonic organization of the inferior parietal convexity of the macaque monkey. *J Comp Neurol* 496: 422–451, 2006. doi:10.1002/cne.20933.
12. **Lewis JW**, **Van Essen DC.** Corticocortical connections of visual, sensorimotor, and multimodal processing areas in the parietal lobe of the macaque monkey. *J Comp Neurol* 428: 112–137, 2000. doi:10.1002/1096-9861(20001204)428:1<112::AID-CNE8>3.0.CO;2-9.
13. **Murray E**, **Coulter J.** Organization of corticospinal neurons in the monkey. *J Comp Neurol* 195: 339–365, 1981. doi:10.1002/cne.901950212.
14. **Padberg J**, **Cooke D**, **Cerkevich C**, **Kaas J**, **Krubitzer L.** Cortical connections of area 2 and posterior parietal area 5 in macaque monkeys. *J Comp Neurol* 527: 718–737, 2019. doi:10.1002/cne.24453.
15. **Pons TP**, **Kaas JH.** Corticocortical connections of area 2 of somatosensory cortex in macaque monkeys: a correlative anatomical and electrophysiological study. *J Comp Neurol* 248: 313–335, 1986. doi:10.1002/cne.902480303.
16. **Seltzer B**, **Pandya DN.** Posterior parietal projections to the intraparietal sulcus of the rhesus monkey. *Exp Brain Res* 62: 459–469, 1986. doi:10.1007/BF00236024.
17. **Vogt B**, **Pandya D.** Cortico-cortical connections of somatic sensory cortex (areas 3, 1 and 2) in the rhesus monkey. *J Comp Neurol* 177: 179–191, 1978. doi:10.1002/cne.901770202.
18. **Gharbawie OA**, **Stepniewska I**, **Qi H**, **Kaas JH.** Multiple parietal-frontal pathways mediate grasping in macaque monkeys. *J Neurosci* 31: 11660–11677, 2011. doi:10.1523/JNEUROSCI.1777-11.2011.
19. **Gnadt JW**, **Andersen RA.** Memory related motor planning activity in posterior parietal cortex of macaque. *Exp Brain Res* 70: 216–220, 1988. doi:10.1007/BF00271862.
20. **Goldring A**, **Cooke D**, **Pineda C**, **Recanzone G**, **Krubitzer L.** Functional characterization of the fronto-parietal reaching and grasping network: reversible deactivation of M1 and areas 2, 5, and 7b in awake behaving monkeys. *J Neurophysiol* 127: 1363–1387, 2022. doi:10.1152/jn.00279.2021.
21. **Heider B**, **Karnik A**, **Ramalingam N**, **Siegel R.** Neural representation during visually guided reaching in macaque posterior parietal cortex. *J Neurophysiol* 104: 3494–3509, 2010. doi:10.1152/jn.01050.2009.
22. **Hyvarinen J**, **Poranen A.** Function of the parietal associative area 7 as revealed from cellular discharges in alert monkeys. *Brain* 97: 673–692, 1974. doi:10.1093/brain/97.1.673.
23. **Ibos G**, **Freedman D.** Interaction between spatial and feature attention in posterior parietal cortex. *Neuron* 91: 931–943, 2016. doi:10.1016/j.neuron.2016.07.025.
24. **Mountcastle VB**, **Lynch JC**, **Georgopoulos A**, **Sakata H**, **Acuna C.** Posterior parietal association cortex of the monkey: command functions for operations within extrapersonal space. *J Neurophysiol* 38: 871–908, 1975. doi:10.1152/jn.1975.38.4.871.
25. **Murata A**, **Gallese V**, **Luppino G**, **Kaseda M**, **Sakata H.** Selectivity for the shape, size, and orientation of objects for grasping in neurons of monkey parietal area AIP. *J Neurophysiol* 83: 2580–2601, 2000. doi:10.1152/jn.2000.83.5.2580.
26. **Orban GA**, **Claeys K**, **Nelissen K**, **Smans R**, **Sunaert S**, **Todd JT**, **Wardak C**, **Durand JB**, **Vanduffel W.** Mapping the parietal cortex of human and non-human primates. *Neuropsychologia* 44: 2647–2667, 2006. doi:10.1016/j.neuropsychologia.2005.11.001.
27. **Rathelot J**, **Dum R**, **Strick P.** Posterior parietal cortex contains a command apparatus for hand movements. *Proc Natl Acad Sci USA* 114: 4255–4260, 2017. doi:10.1073/pnas.1608132114.
28. **Seelke A**, **Padberg J**, **Disbrow E**, **Purnell S**, **Recanzone G**, **Krubitzer L.** Topographic maps within Brodmann's area 5 of macaque monkeys. *Cereb Cortex* 22: 1834–1850, 2012. doi:10.1093/cercor/bhr257.
29. **Baldwin M**, **Cooke D**, **Goldring A**, **Krubitzer L.** Representations of fine digit movements in posterior and anterior parietal cortex revealed using long-train intracortical microstimulation in macaque monkeys. *Cereb Cortex* 28: 4244–4263, 2018. doi:10.1093/cercor/bhx279.
30. **Burish M**, **Stepniewska I**, **Kaas J.** Microstimulation and architectonics of frontoparietal cortex in common marmosets (*Callithrix jacchus*). *J Comp Neurol* 507: 1151–1168, 2008. doi:10.1002/cne.21596.
31. **Mayer A**, **Baldwin M**, **Cooke D**, **Lima B**, **Padberg J**, **Lewenfus G**, **Franca JG**, **Krubitzer L.** The multiple representations of complex digit movements in primary motor cortex form the building blocks for complex grip types in capuchin monkeys. *J Neurosci* 39: 6684–6695, 2019. doi:10.1523/JNEUROSCI.0556-19.2019.
32. **Baldwin MKL**, **Cooke DF**, **Krubitzer L.** Intracortical microstimulation maps of motor, somatosensory, and posterior parietal cortex in tree shrews (*Tupaia belangeri*) reveal complex movement representations. *Cereb Cortex* 27: 1439–1456, 2017. doi:10.1093/cercor/bhv329.
33. **Halley A**, **Baldwin M**, **Cooke D**, **Englund M**, **Krubitzer L.** Distributed motor control of limb movements in rat motor and somatosensory cortex: the sensorimotor amalgam revisited. *Cereb Cortex* 30: 6296–6312, 2020. doi:10.1093/cercor/bhaa186.
34. **Matyas F**, **Sreenivasan V**, **Marbach F**, **Wacongne C**, **Barsy B**, **Mateo C**, **Aronoff R**, **Petersen CCH.** Motor control by sensory cortex. *Science* 330: 1240–1243, 2010. doi:10.1126/science.1195797.
35. **Halley A**, **Baldwin M**, **Cooke D**, **Englund M**, **Pineda C**, **Schmid T**, **Yartsev MM**, **Krubitzer L.** Coevolution of motor cortex and behavioral specializations associated with flight and echolocation in bats. *Curr Biol* 32: 2935–2941.e3, 2022. doi:10.1016/j.cub.2022.04.094.
36. **Sreenivasan V**, **Karmakar K**, **Rijli F**, **Petersen C.** Parallel pathways from motor and somatosensory cortex for controlling whisker movements in mice. *Eur J Neurosci* 41: 354–367, 2015. doi:10.1111/ejn.12800.
37. **Nudo RJ**, **Masterton RB.** Descending pathways to the spinal cord, III: Sites of origin of the corticospinal tract. *J Comp Neurol* 296: 559–583, 1990. doi:10.1002/cne.902960405.
38. **Welniarz Q**, **Dusart I**, **Roze E.** The corticospinal tract: evolution, development, and human disorders: corticospinal tract human disorders. *Dev Neurobiol* 77: 810–829, 2017. doi:10.1002/dneu.22455.
39. **Mao T**, **Kusefoglu D**, **Hooks B**, **Huber D**, **Petreanu L**, **Svoboda K.** Long-range neuronal circuits underlying the interaction between sensory and motor cortex. *Neuron* 72: 111–123, 2011. doi:10.1016/j.neuron.2011.07.029.
40. **Porter LL**, **White EL.** Afferent and efferent pathways of the vibrissal region of primary motor cortex in the mouse. *J Comp Neurol* 214: 279–289, 1983. doi:10.1002/cne.902140306.
41. **Smith JB**, **Alloway KD.** Rat whisker motor cortex is subdivided into sensory-input and motor-output areas. *Front Neural Circuits* 7: 4, 2013. doi:10.3389/fncir.2013.00004.
42. **Jones EG**, **Coulter JD**, **Hendry SHC.** Intracortical connectivity of architectonic fields in the somatic sensory, motor and parietal cortex of monkeys. *J Comp Neurol* 181: 291–347, 1978. doi:10.1002/cne.901810206.
43. **Goldring A**, **Cooke D**, **Baldwin M**, **Recanzone G**, **Gordon A**, **Pan T**, **Simon SI**, **Krubitzer L.** Reversible deactivation of higher-order posterior parietal areas. II. Alterations in response properties of neurons in areas 1 and 2. *J Neurophysiol* 112: 2545–2560, 2014. doi:10.1152/jn.00141.2014.
44. **Caminiti R**, **Borra E**, **Visco-Comandini F**, **Battaglia-Mayer A**, **Averbeck BB**, **Luppino G.** Computational architecture of the parieto-frontal network underlying cognitive-motor control in monkeys. *eNeuro* 4: ENEURO.0306-16.2017, 2017. doi:10.1523/ENEURO.0306-16.2017.
45. **Klam F**, **Graf W.** Discrimination between active and passive head movements by macaque ventral and medial intraparietal cortex neurons. *J Physiol* 574: 367–386, 2006. doi:10.1113/jphysiol.2005.103697.
46. **Bonazzi L**, **Viaro R**, **Lodi E**, **Canto R**, **Bonifazzi C**, **Franchi G.** Complex movement topography and extrinsic space representation in the rat forelimb motor cortex as defined by long-duration intracortical microstimulation. *J Neurosci* 33: 2097–2107, 2013. doi:10.1523/JNEUROSCI.3454-12.2013.
47. **Cooke DF**, **Graziano MSA.** Sensorimotor integration in the precentral cyrus: polysensory neurons and defensive movements. *J Neurophysiol* 91: 1648–1660, 2004. doi:10.1152/jn.00955.2003.
48. **Hall RD**, **Lindholm EP.** Organization of motor and somatosensory neocortex in the albino rat. *Brain Res* 66: 23–38, 1974. doi:10.1016/0006-8993(74)90076-6.
49. **Cooke D**, **Goldring A**, **Yamayoshi I**, **Tsourkas P**, **Recanzone G**, **Tiriac A**, **Pan T**, **Simon SI**, **Krubitzer L.** Fabrication of an inexpensive, implantable cooling device for reversible brain deactivation in animals ranging from rodents to primates. *J Neurophysiol* 107: 3543–3558, 2012. doi:10.1152/jn.01101.2011.
50. **Cooke DF**, **Goldring AB**, **Baldwin MKL**, **Recanzone GH**, **Chen A**, **Pan T**, **Simon SI**, **Krubitzer L.** Reversible deactivation of higher-

order posterior parietal areas. I. Alterations of receptive field characteristics in early stages of neocortical processing. *J Neurophysiol* 112: 2529–2544, 2014. doi:10.1152/jn.00140.2014.

51. **Schindelin J**, **Arganda-Carreras I**, **Frise E**, **Kaynig V**, **Longair M**, **Pietzsch T**, **Preibisch S**, **Rueden C**, **Saalfeld S**, **Schmid B**, **Tinevez JY**, **White DJ**, **Hartenstein V**, **Eliceiri K**, **Tomancak P**, **Cardona A.** Fiji: an open-source platform for biological-image analysis. *Nat Methods* 9: 676–682, 2012. doi:10.1038/nmeth.2019.
52. **Thier P**, **Andersen R.** Electrical microstimulation distinguishes distinct saccade-related areas in the posterior parietal cortex. *J Neurophysiol* 80: 1713–1735, 1998. doi:10.1152/jn.1998.80.4.1713.
53. **Rozzi S**, **Ferrari PF**, **Bonini L**, **Rizzolatti G**, **Fogassi L.** Functional organization of inferior parietal lobule convexity in the macaque monkey: electrophysiological characterization of motor, sensory and mirror responses and their correlation with cytoarchitectonic areas. *Eur J Neurosci* 28: 1569–1588, 2008. doi:10.1111/j.1460-9568.2008.06395.x.
54. **Cardillo G.** MyFisher: the definitive function for the Fisher's exact and conditional test for any RxC matrix. 2023. http://www.mathworks.com/matlabcentral/fileexchange/26883 [2023 July 17].
55. **Rubin M.** Do p values lose their meaning in exploratory analyses? It depends how you define the familywise error rate. *Rev Gen Psychol* 21: 269–275, 2017. doi:10.1037/gpr0000123.
56. **Caminiti R**, **Innocenti G**, **Battaglia-Mayer A.** Organization and evolution of parieto-frontal processing streams in macaque monkeys and humans. *Neurosci Biobehav Rev* 56: 73–96, 2015. doi:10.1016/j.neubiorev.2015.06.014.
57. **Stepniewska I**, **Friedman RM**, **Gharbawie OA**, **Cerkevich CM**, **Roe AW**, **Kaas JH.** Optical imaging in galagos reveals parietal-frontal circuits underlying motor behavior. *Proc Natl Acad Sci USA* 108: E725–E732, 2011. doi:10.1073/pnas.1109925108.
58. **Sherman SM.** Thalamus plays a central role in ongoing cortical functioning. *Nat Neurosci* 19: 533–541, 2016. doi:10.1038/nn.4269.
59. **Bostan AC**, **Dum RP**, **Strick PL.** Functional anatomy of basal ganglia circuits with the cerebral cortex and the cerebellum. *Prog Neurol Surg* 33: 50–61, 2018. doi:10.1159/000480748.
60. **Stepniewska I**, **Friedman R**, **Miller D**, **Kaas J.** Interactions within and between parallel parietal-frontal networks involved in complex motor behaviors in prosimian galagos and a squirrel monkey. *J Neurophysiol* 123: 34–56, 2020. doi:10.1152/jn.00576.2019.
61. **Baldwin MKL**, **Cooke DF**, **Gordon AG**, **Krubitzer LA.** Revealing functional organization of frontoparietal networks in tree shrews (*Tupaia belangeri*) using reversible inactivation (Abstract). *Soc Neurosci Abstr* 40: 446.02, 2014. https://www.abstractsonline.com/Plan/ViewAbstract.aspx?sKey=29a54d34-b73c-4003-ba28-3e9b0855a22d&cKey=a46e7465-42b0-4559-b38b-3e7a766beb2d&mKey=%7b54C85D94-6D69-4B09-AFAA-502C0E680CA7%7d.
62. **Delhaye B**, **Long K**, **Bensmaia S.** Neural basis of touch and proprioception in primate cortex. *Compr Physiol* 8: 1575–1602, 2019. doi:10.1002/cphy.c170033.
63. **Padberg J**, **Cerkevich C**, **Engle J**, **Rajan AT**, **Recanzone G**, **Kaas J**, **Krubitzer L.** Thalamocortical connections of parietal somatosensory cortical fields in macaque monkeys are highly divergent and convergent. *Cereb Cortex* 19: 2038–2064, 2009. doi:10.1093/cercor/bhn229.
64. **Rausell E**, **Bickford L**, **Manger PR**, **Woods TM**, **Jones EG.** Extensive divergence and convergence in the thalamocortical projection to monkey somatosensory cortex. *J Neurosci* 18: 4216–4232, 1998. doi:10.1523/JNEUROSCI.18-11-04216.1998.
65. **Burton H**, **Fabri M.** Ipsilateral intracortical connections of physiologically defined cutaneous representations in areas 3b and 1 of macaque monkeys: projections in the vicinity of the central sulcus. *J Comp Neurol* 355: 508–538, 1995. doi:10.1002/cne.903550404.
66. **Stepniewska I**, **Preuss T**, **Kaas J.** Architectionis, somatotopic organization, and ipsilateral cortical connections of the primary motor area (M1) of owl monkeys. *J Comp Neurol* 330: 238–271, 1993. doi:10.1002/cne.903300207.
67. **Dea M**, **Hamadjida A**, **Elgbeili G**, **Quessy S**, **Dancause N.** Different patterns of cortical Inputs to subregions of the primary motor cortex hand representation in *Cebus apella*. *Cereb Cortex* 26: 1747–1761, 2016. doi:10.1093/cercor/bhv324.
68. **Jeffers MS**, **Touvykine B**, **Ripley A**, **Lahey G**, **Carter A**, **Dancause N**, **Corbett D.** Poststroke impairment and recovery are predicted by task-specific regionalization of injury. *J Neurosci* 40: 6082–6097, 2020. doi:10.1523/JNEUROSCI.0057-20.2020.
69. **O'Connor DH**, **Krubitzer L**, **Bensmaia S.** Of mice and monkeys: somatosensory processing in two prominent animal models. *Prog Neurobiol* 201: 102008, 2021. doi:10.1016/j.pneurobio.2021.102008.